Preprints of the 21st IFAC World Congress (Virtual)
Berlin, Germany, July 12-17, 2020

Droop-Based Two-Layer Cooperation for Multiple DC Microgrid Clusters

Xiaoqing Lu * **Jingang Lai** **

* *School of Electrical Engineering and Automation, Wuhan University, Wuhan 430072, China (e-mail: luxq@whu.edu.cn).*
** *E.ON Energy Research Center, RWTH Aachen University, Aachen 52074, Germany (e-mail: jinganglai@126.com)*

Abstract: Enabling energy exchange among multiple dc microgrids (MGs) and adjusting the current outputs of all converters proportional to their power capacities can significantly improve power supply reliability as well as effectively avoid overloaded or uncertainty. By dividing all converters within each dc MG cluster into the leader-converters and follower-converters according to their physical cluster topology structure, the leader and follower control layers are respectively formulated. Then a droop-based two-layer cooperative strategy is developed, under which the weighted average voltage of all converters can be regulated to their rated references, meanwhile, the accurate current sharing can be simultaneously realized not only within each dc MG but also among multiple dc MG clusters. All controllers are fully distributed and can be applied in all sparse two-layer cyber networks, control time constant related sufficient conditions are also derived to ensure the whole system stability. The effectiveness of the results are verified through different cases in MATLAB/SimPowerSystems.

Keywords: two-layer cooperation, current sharing, voltage regulation, dc microgirds.

1. INTRODUCTION

Recent years have witnessed much attention to dc MGs due to their increased efficiency in delivering power and flexibility for the integration of power sources with dc nature (e.g., photovoltaic and battery energy storage systems). As one of the major control objectives, proper voltage regulation while satisfying the proportional current sharing among all converters, i.e., power allocation among converters based on their current ratings, within each dc MG is of paramount value [Yu (2016)].

Among all the vast hierarchical control approaches [Guerrero (2011)], droop control, as a local and communication-free method, is widely adopted to realize the mentioned two control objectives in a decentralized manner, although it is inherently incapable of achieving accurate current sharing and voltage regulation simultaneously [Zhong (2011), Huang (2015), Lai (2016)]. Thus distributed secondary controls generally need to be implemented to eliminate the previous control deviations, respectively due to its better robustness against the single point failure and control performance to invoke system sources than the centralized and decentralized ones [Lu (2018)].

Recently, many distributed secondary control methods for single dc MGs have been proposed, including the voltage regulation [Farag (2012), Dam (2018)], current sharing [Tucci (2018), Guo (2018), Cucuzzella (2018)], and the stability analysis in the situation of communication delay [Dong (2019)] and switching communication network [Lai (2019)]. While a number of neighbouring single dc MGs are prone to being connected in a certain region due to the large-scale development of the dc MGs. Whenever some dc MGs have an excess of power while others have a need for power, it might be beneficial for these dc MGs (and their consumers) to exchange energy with one another instead of requesting it from the main grid. This energy exchange between nearby dc MGs can not only significantly reduce the amount of power that is wasted during the transmission over the distribution lines, but also enhance the autonomy of the MG system while reducing the demand and reliance on the main grid.

It is thus of interest to devise a cooperative strategy to enable such a local energy trade between dc MG clusters that are in need of energy, nevertheless, controlling the energy exchange among multiple dc MG clusters has not received sufficient attention yet. So far the associated cooperative approaches on multiple MG clusters include the tie-line current and the loading data-based voltage reference regulation methods for multiple dc MG clusters [Shafiee (2014), Moayedi (2016)], the cooperative strategy for grid-connected ac MGs [Maknouninejad (2012)], and the droop-based power management and cluster-oriented accurate power sharing strategies for multiple ac MG clusters [Nutkani (2013), Lu (2018), Lai (2019)]. To this end, multiple dc MG cluster-oriented cooperative strategies for regulating the system voltage and the current sharing of the electronically-interfaced converters are necessary for reliable operation of multiple dc MG clusters.

Taking into account all the aforementioned problems, this paper develops a droop-based two-layer cooperative strategy, consisting of the leader-converter control (LCC) scheme and the follower-converter control (FCC) scheme, for multiple dc MG clusters. The converters near some critical points (e.g., the downstream point in a feeder or the sampling point of the underload transformer tap changer) within each dc MG cluster are selected as the leader-converters located in the upper control layer, whereas others as the follower-converters located in the lower control layer. The FCC scheme enables all follower-converters within each dc MG cluster to track the operation states of their respective leader-converter, which are then driven to the expected reference states by the LCC scheme. Then all the state errors across the two-layer cyber network are fed back to the primary control process so as to adjust all converters' voltage nominal set-points. The main contributions are as follows.

(i) Different from most existing current sharing methods [Tucci (2018), Guo (2018), Cucuzzella (2018)], this paper designs the two-layer voltage estimators, through which the voltage estimates of all follower-converters within each MG cluster can be synchronized to that of their respective leader-converters, simultaneously the voltage estimates of all leader-converters can be driven to the rated voltage reference. Then all converters' voltages can be finally converged to an acceptable range, which in turn leads to the realization of accurate current sharing not only within each MG cluster but also among multiple MG clusters.

(ii) The proposed strategy enables the energy exchange among multiple MG clusters, generally occurred in the tertiary control process, to be completed only through secondary control by directly feeding back the current sharing mismatches across the leader and follower control layers into the primary control. The associated time consumption of energy exchange can be significantly reduced, which becomes much apparent for MG clusters containing a large amount of heterogenous converters [Apostolopoulou (2014)]. Thus, the results are different from most works on islanded dc MGs [Farag (2012), Dam (2018)] and dc MG clusters [Shafiee (2014), Moayedi (2016)].

(iii) Different from the existing results [Huang (2015), Nasirian (2016), Dong (2019)], by using the tools of algebraic graph theory and special matrix theory, the whole system stability can be guaranteed as long as the control time constant of the follower-converters is less than that of the leader-converters. It reflects the fact that the energy flow within each MG cluster change faster than that among multiple MG clusters, which further indicates that the established sparse two-layer cyber network well fits the physical cluster topology structure of the multiple dc MGs. Besides the faster convergence performance compared to existing single-layer networks [Lai (2016), Lu (2018)], the proposed strategy enables the distributed power transfer among MG clusters to avoid overloaded or uncertainty.

The remaining part is organized as follows. Sec. II formulates the two-layer cyber network, and the main cooperative strategy and the stability analysis are presented in Sec. III, which will be verified by simulations given in Sec. IV. Sec. V finally concludes this paper.

Throughout this paper let I_N be the $N \times N$ identity matrix, $\otimes$ be the Kronecker Product, $1_N = (1, \cdots, 1)^T$, $\mathcal{I}_M = \{1, \cdots, M\}$, $\mathcal{I}_{n_k} = \{1, \cdots, n_k\}$. For symmetric matrix A, denote $\lambda_{\max}(A)$, $\lambda_{\min}(A)$, and $\lambda_2(A)$, respectively, the maximum, minimum, and the second minimum eigenvalues of A.

2. TWO-LAYER CYBER NETWORK

Consider a multiple dc MG cluster system containing M dc MG clusters labeled $\mathrm{MG}_1, \cdots, \mathrm{MG}_M$. All converters within the kth MG cluster, MG_k, are divided into one leader-converter labeled $(k, 0)$ and n_k follower-converters labeled $(k, 1), \cdots, (k, n_k)$.

All follower-converters from MG_k, constitute the kth lower control layer, which are permitted to exchange information within MG_k across the kth lower cyber network, $\mathcal{G}_k$. The associated interconnection topology is described by the digraph $\mathcal{G}_k(\mathcal{V}_k, \mathcal{E}_k, A_k)$ with the follower-converter node set $\mathcal{V}_k = \{\mathcal{V}_{k,1}, \cdots, \mathcal{V}_{k,n_k}\}$, cyber link set $\mathcal{E}_k \subseteq \mathcal{V}_k \times \mathcal{V}_k$, and the adjacency matrix $A_k = (a_{ij}^k)_{(n_k)\times(n_k)}$ ($a_{ii}^k = 0$ and $a_{ij}^k \geq 0$), where $a_{ij}^k > 0$ if and only if the edge $(\mathcal{V}_{k,i}, \mathcal{V}_{k,j}) \in \mathcal{E}_k$. The neighbor set of $\mathrm{CV}_{k,i}$ is given by $N_{k,i} = \{\mathcal{V}_{k,j} \in \mathcal{V}_k : (\mathcal{V}_{k,i}, \mathcal{V}_{k,j}) \in \mathcal{E}_k\}$. The leader-adjacency matrix $B_k = \mathrm{diag}\{a_{10}^k, \cdots, a_{n_k 0}^k\}$ is used to describe the interconnection topology between the leader-converter $\mathrm{CV}_{k,0}$ and n_k follower-converter $\mathrm{CV}_{k,i}$ ($i \in \mathcal{I}_{n_k}$), where $a_{i0}^k > 0$ if $\mathrm{CV}_{k,i}$ is connected to $\mathrm{CV}_{k,0}$ through the cyber link $(\mathcal{V}_{k,i}, \mathcal{V}_{k,0})$, otherwise $a_{i0}^k = 0$.

All leader-converters constitute the upper control layer, which are allowed to exchange information among multiple MG clusters through the upper cyber network $\tilde{\mathcal{G}}$. The associated interconnection topology is described by the digraph $\tilde{\mathcal{G}}(\tilde{\mathcal{V}}, \tilde{\mathcal{E}}, \tilde{A})$ with the leader-converter node set $\tilde{\mathcal{V}} = \{\mathcal{V}_{1,0}, \cdots, \mathcal{V}_{M,0}\}$, communication link set $\tilde{\mathcal{E}} \subseteq \tilde{\mathcal{V}} \times \tilde{\mathcal{V}}$, and adjacency matrix $\tilde{A} = (\tilde{a}_{k\ell})_{M\times M}$. The neighbor set of $\mathrm{CV}_{k,0}$ is $\tilde{N}_k = \{\tilde{\mathcal{V}}_\ell \in \tilde{\mathcal{V}} : (\tilde{\mathcal{V}}_k, \tilde{\mathcal{V}}_\ell) \in \tilde{\mathcal{E}}\}$. Moreover, to regulate the voltage of each $\mathrm{CV}_{k,0}$ after the current sharing within MG_k is achieved, we then introduce the leader-adjacency matrix $\tilde{B} = \mathrm{diag}\{\tilde{a}_{10}, \cdots, \tilde{a}_{M0}\}$ with $\tilde{a}_{k0} > 0$ ($k \in \mathcal{I}_M$) if the rated voltage reference, v^{rated}, is available to the leader-converter $\mathrm{CV}_{k,0}$, otherwise $\tilde{a}_{k0} = 0$.

Assume the two-layer cyber network satisfies the connectivity condition. Further suppose all $\{\mathcal{G}_k\}_{k=1}^M$ and $\tilde{\mathcal{G}}$ are detailed-balanced with positive vectors ς_k and $\tilde{\varsigma}$, respectively. Thus, $\mathrm{diag}(\varsigma_k)L_k + B_k$ and $\mathrm{diag}(\tilde{\varsigma})\tilde{L} + \tilde{B}$ are positive definite with Laplacian matrices L_k and $\tilde{L}$ corresponding to A_k and $\tilde{A}$, respectively.

3. DROOP-BASED TWO-LAYER COOPERATIVE STRATEGY

The proposed strategy includes the following primary control process, follower-converter control scheme, and leader-converter control scheme, which follows the corresponding stability analysis.

For the kth MG cluster, droop control is locally employed to realize the current sharing among all converters within MG_k. Then the output voltage of the ith converter in MG_k, $\mathrm{CV}_{k,i}$, follows the droop principle,

$$v_{k,i} = v_{k,i}^{\mathrm{nom}} - g_{k,i} i_{k,i}, \tag{1}$$

with the voltage nominal set-point $v_{k,i}^{\mathrm{nom}}$, the droop gain $g_{k,i}$, and the output current $i_{k,i}$ of $\mathrm{CV}_{k,i}$.

Since each dc MG consists of power converters connected through different line impedances, tuning of the voltage controller provides a simple and intuitive tradeoff between the conflicting goals of voltage regulation and current sharing. To ensure accurate current sharing, the FCC scheme should synchronize the weighted average voltage of all follower-converters to that of their respective leader-converters, and the LCC scheme then drives the weighted average voltage of all leader-converters to the rated voltage reference. Accordingly, the objectives are to regulate $v_{k,i}^{\text{nom}}$ in (1) such that for all $i \in \mathcal{I}_{n_k}$ and $k \neq \ell \in \mathcal{I}_M$,

$$\begin{aligned} &\lim_{t\to\infty} \left|\sum_{i=1}^{n_k} \mu_{k,i} v_{k,i}(t) - \sum_{k=1}^{M} \tilde{\mu}_k v_{k,0}(t)\right| = 0, \\ &\lim_{t\to\infty} \left|i_{k,i}(t)/i_{k,i}^{\max} - i_{k,0}(t)/i_{k,0}^{\max}\right| = 0, \end{aligned} \tag{2}$$

$$\begin{aligned} &\lim_{t\to\infty} \left|\sum_{k=1}^{M} \tilde{\mu}_k v_{k,0}(t) - v^{\text{rated}}\right| = 0, \\ &\lim_{t\to\infty} \left|i_{k,0}(t)/i_{k,0}^{\max} - i_{\ell,0}(t)/i_{\ell,0}^{\max}\right| = 0, \end{aligned} \tag{3}$$

where $\mu_k = (\mu_{k,1}, \cdots, \mu_{k,n_k})^T \in R^{n_k}$, $\tilde{\mu} = (\tilde{\mu}_1, \cdots, \tilde{\mu}_M)^T \in R^M$ are the normalized positive left eigenvectors for the zero eigenvalues of the semi-positive matrices $\text{diag}(\varsigma_k)L_k$ and $\text{diag}(\tilde{\varsigma})\tilde{L}$ (associated with $\mathcal{G}_k$ and $\tilde{\mathcal{G}}$); $i_{k,i}^{\max}$ and $i_{k,0}^{\max}$ are the maximum current outputs of $\text{CV}_{k,i}$ and $\text{CV}_{k,0}$, respectively. Note that $\mu_k = (1/n_k, \cdots, 1/n_k)^T$ and $\tilde{\mu} = (\frac{1}{M}, ..., \frac{1}{M})$ if $\mathcal{G}_k$ and $\tilde{\mathcal{G}}$ are detail-balanced with ς_k and $\tilde{\varsigma}$.

3.1 Two-Layer Voltage Estimators

Due to the conflict between precise voltage regulation and accurate current sharing in dc MGs, we adopt a compromise method to regulate the weighted average voltage of all converters to an acceptable range. To this end, we first design the two-layer voltage estimators as:

$$\begin{aligned} &\hat{v}_{k,i}(t) = v_{k,i}(t) + \int_{t_0}^{t} \sum_{j\in N_{k,i}} \varsigma_{k,i} a_{ij}^k \left[\hat{v}_{k,j}(s) - \hat{v}_{k,i}(s)\right] \mathrm{d}s, \\ &\tilde{v}_{k,0} = v_{k,0} + \int_{t_0}^{t} \sum_{\ell\in \tilde{N}_k} \tilde{\varsigma}_k \tilde{a}_{k\ell} [\tilde{v}_{\ell,0}(s) - \tilde{v}_{k,0}(s)] \mathrm{d}s, \end{aligned} \tag{4}$$

where $\hat{v}_{k,i}$ and $\tilde{v}_{k,0}$ are the estimates of the measured voltage $v_{k,i}$ and $v_{k,0}$, associated with the follower-converter $\text{CV}_{k,i}$ and leader-converter $\text{CV}_{k,0}$ with $i \in \mathcal{I}_{n_k}$ and $k \in \mathcal{I}_M$. Based on (4), any voltage deviations across $\mathcal{G}_k$ and $\tilde{\mathcal{G}}$ can be directly estimated in a distributed way, which makes the global voltage information (involving centralized control) is unnecessary for each converter.

3.2 Follower-Converter Control Scheme

Since all follower-converters within MG_k can communicate with their neighbors through a sparse lower layer network, $\mathcal{G}_k$, the pinning-based voltage and current controllers can be designed as

$$\begin{cases} \tau \dot{\hat{v}}_{k,i} = \sum_{j\in N_{k,i}} a_{ij}^k [\hat{v}_{k,j} - \hat{v}_{k,i}] + a_{i0}^k [\tilde{v}_{k,0} - \hat{v}_{k,i}], \\ \tau \dot{i}_{k,i} = \sum_{j\in N_{k,i}} a_{ij}^k [g_{k,j} i_{k,j} - g_{k,i} i_{k,i}]/g_{k,i} \\ \qquad + a_{i0}^k [g_{k,0} i_{k,0} - g_{k,i} i_{k,i}]/g_{k,i}, \end{cases} \tag{5}$$

for $i \in \mathcal{I}_{n_k}$. $\text{CV}_{k,i}$ can access the synchronization states of its leader-converter, $\tilde{v}_{k,0}$ and $i_{k,0}$, if and only when $a_{i0}^k > 0$. The time constant τ, representing the response speed of the follower-converter control layer, will be determined later. Based on (5), the weighted average voltage and current output ratios of all follower-converters, $\hat{v}_{k,i}$ and $i_{k,i}/i_{k,i}^{\max}$, can be synchronized to that of their respective leader-converters, $\tilde{v}_{k,0}$ and $i_{k,0}/i_{k,0}^{\max}$.

3.3 Leader-Converter Control Scheme

Since all leader-converters from each MG cluster can communicate with their neighbors through a sparse upper layer network, $\tilde{\mathcal{G}}$, the pinning-based voltage and consensus-based current controllers can be designed as

$$\begin{cases} T\dot{\tilde{v}}_{k,0} = \sum_{\ell\in \tilde{N}_k} \tilde{a}_{k\ell}^k [\tilde{v}_{\ell,0} - \tilde{v}_{k,0}] + \tilde{a}_{k0} [v^{\text{rated}} - \tilde{v}_{k,0}]. \\ T\dot{i}_{k,0} = \sum_{\ell\in \tilde{N}_k} \tilde{a}_{k\ell} [g_{\ell,0} i_{\ell,0} - g_{k,0} i_{k,0}]/g_{k,0}, \end{cases} \tag{6}$$

where MG_k can access v^{rated} if and only when $\tilde{a}_{k0} > 0$, and $T > 0$ is the time constant of the leader-converter control layer. Based on (6), the weighted average voltage of all leader-converters, $\tilde{v}_{k,0}$, can be synchronized to the rated reference, v^{rated}, meanwhile their current output ratios will be equal, i.e., $i_{k,0}/i_{k,0}^{\max} = i_{\ell,0}/i_{\ell,0}^{\max}$ for all $k \neq \ell \in \mathcal{I}_M$.

3.4 Stability Analysis

First we prove the stability of the proposed two-layer voltage estimators (4). Denote $\hat{v}_k = (\hat{v}_{k,1}, \cdots, \hat{v}_{k,n_k})^T$, and $\tilde{v} = (\tilde{v}_1^T, \cdots, \tilde{v}_M^T)^T$. Differentiating both sides of (4) yields

$$\begin{aligned} \dot{\hat{v}}_k(t) &= \dot{v}_k(t) - \text{diag}(\varsigma_k) L_k \hat{v}_k(t), \\ \dot{\tilde{v}}_0(t) &= \dot{v}_0(t) - \text{diag}(\tilde{\varsigma}) \tilde{L} \tilde{v}_0(t), \end{aligned} \tag{7}$$

which can be rewritten in the frequency domain

$$\begin{aligned} \hat{V}_k(s) &= s(sI_{n_k} + \text{diag}(\varsigma_k) L_k)^{-1} V_k(s), \\ \tilde{V}_0(s) &= s(sI_M + \text{diag}(\tilde{\varsigma}) \tilde{L})^{-1} V_0(s), \end{aligned} \tag{8}$$

where $\hat{V}_k$, $\tilde{V}_0$, V_k, and V_0, are the Laplace transforms of $\hat{v}_k$, $\tilde{v}_0$, v_k, and v_0, respectively. If $\mathcal{G}_k$ and $\tilde{\mathcal{G}}$, are detail-balanced and connected, then $\text{diag}(\varsigma_k)L_k$ and $\text{diag}(\tilde{\varsigma})\tilde{L}$ are irreducible. By the Nyquist stability criterion, the transfer functions $s(sI_{n_k} + \text{diag}(\varsigma_k)L_k)^{-1}$ and $s(sI_M + \text{diag}(\tilde{\varsigma})\tilde{L})^{-1}$ are stable [Olfati-Saber (2004)]. Moreover, $\sum_{i=1}^{n_k} \mu_{k,i} v_{k,i}(t)$ and $\sum_{k=1}^{M} \tilde{\mu}_k v_{k,0}(t)$ are invariant quantities, respectively, for positive left eigenvectors ς_k and $\tilde{\varsigma}$, this together with the final value theorem give:

$$\begin{aligned} \lim_{t\to\infty} \sum_{i=1}^{n_k} \mu_{k,i} v_{k,i}(t) &= \lim_{t\to\infty} \hat{v}_k(t), \\ \lim_{t\to\infty} \sum_{k=1}^{M} \tilde{\mu}_k v_{k,0}(t) &= \lim_{t\to\infty} \tilde{v}_0(t). \end{aligned} \tag{9}$$

Hence we conclude that the voltage estimators (4) can steer all converters' voltage estimates to asymptotically converge to the weighted average value of all converters' actual voltage magnitudes.

Next we present the stability of the proposed two-layer cooperative strategy with FCC scheme (5) and LCC scheme (6). To facilitate the mathematical representation, we suppose the number of follower-converters in each MG cluster is equal to n, whereas the general case can be analyzed similarly. Now let $\hat{v} = (\hat{v}_1^T, \cdots, \hat{v}_M^T)^T$, $\eta_{k,i} = g_{k,i} i_{k,i}$, $\eta_k = (\eta_{k,1}, \cdots, \eta_{k,n})^T$, $\eta = (\eta_1^T, \cdots, \eta_M^T)^T$, $\varsigma = (\varsigma_1^T, \cdots, \varsigma_n^T)^T$, $L = \text{diag}\{L_1, \cdots, L_M\}$, and $B = \text{diag}(B_1, \cdots, B_M)$. Moreover, denote $\eta_0 = (\eta_{1,0}, \cdots, \eta_{M,0})^T$. Denote the error variables: $\bar{v} = \hat{v} - \tilde{v}_0(t) \otimes 1_n$, $\bar{\eta} = \eta - \eta_0 \otimes 1_n$, $\bar{v}_0 = \hat{v}_0 - v^{\text{rated}} \otimes 1_M$, and $\bar{\eta}_0 = \eta_0 - \tilde{\mu}^T \eta_0(0)$, then the error dynamics of (5) and (6) under estimators (4) can be derived as

$$\begin{cases} \tau \dot{\bar{v}} = -(\text{diag}(\varsigma) L + B) \bar{v} + \frac{\tau}{T} [(\text{diag}(\tilde{\varsigma}) \tilde{L} + \tilde{B}) \bar{v}_0] \otimes 1_n, \\ T \dot{\bar{v}}_0 = -(\text{diag}(\tilde{\varsigma}) \tilde{L} + \tilde{B}) \bar{v}_0, \\ \tau \dot{\bar{\eta}} = -(\text{diag}(\varsigma) L + B) \bar{\eta} + \frac{\tau}{T} (\tilde{L} \bar{\eta}_0) \otimes 1_n, \\ T \dot{\bar{\eta}}_0 = -\text{diag}(\tilde{\varsigma}) \tilde{L} \bar{\eta}_0. \end{cases} \tag{10}$$

Define the Lyapunov candidates $V = \frac{1}{2}\varsigma^T\varsigma$ with $\varsigma = [\bar{v}^T, (\bar{v}_0 \otimes 1_n)^T, \bar{\eta}^T, (\bar{\eta}_0 \otimes 1_n)^T]$ and differentiate along the trajectory of system (10), we have

$$\begin{aligned} \dot{V}\Big|_{(10)} \leq & -[\tfrac{2}{\tau}\lambda_{\min}(\mathrm{diag}(\varsigma)L + B) - \gamma](\bar{v}^T\bar{v} + \bar{\eta}^T\bar{\eta}) \\ & -\tfrac{2}{T}\lambda_{\min}(\mathrm{diag}(\tilde{\varsigma})\tilde{L} + \tilde{B})\bar{v}_0^T\bar{v}_0 \\ & +\tfrac{1}{\gamma T^2}\lambda_{\max}([\mathrm{diag}(\tilde{\varsigma})\tilde{L} + \tilde{B}]^2)\bar{v}_0^T\bar{v}_0 \\ & -[\tfrac{2}{T}\lambda_2(\mathrm{diag}(\tilde{\varsigma})\tilde{L}) - \tfrac{1}{\gamma T^2}\lambda_{\max}([\mathrm{diag}(\tilde{\varsigma})\tilde{L}]^2)]\bar{\eta}_0^T\bar{\eta}_0, \end{aligned} \tag{11}$$

where γ is an arbitrary positive constant. Hence, a sufficient condition for $\dot{V}(t)|_{(10)} < 0$ is

$$\frac{\tau}{T} < \min\left\{\frac{4\lambda_{\min}(\mathrm{diag}(\varsigma)L+B)\lambda_2(\tilde{L})}{\lambda_{\max}([\mathrm{diag}(\tilde{\varsigma})\tilde{L}]^2)}, \frac{4\lambda_{\min}(\mathrm{diag}(\varsigma)L+B)\lambda_{\min}(\mathrm{diag}(\tilde{\varsigma})\tilde{L}+\tilde{B})}{\lambda_{\max}([\mathrm{diag}(\tilde{\varsigma})\tilde{L}+\tilde{B}]^2)}\right\} \triangleq \vartheta. \tag{12}$$

Note that once $g_{k,i}i_{k,i} \to g_{k,0}i_{k,0}$ for all $i \in \mathcal{I}_{n_k}$ and $k \in \mathcal{I}_M$, the current sharing objectives in (2) and (3) can be realized. Now we can obtain the following conclusion.

Conclusion: Suppose the two-layer cyber networks, $\{\mathcal{G}_k\}_{k=1}^M$ and $\tilde{\mathcal{G}}$, are detail-balanced and connected. If the control time constants satisfy condition (12), then the voltage regulation and current sharing objectives (2) and (3) can be achieved provided that each MG cluster selects at least one leader-converter to realize the information exchange among all MG clusters and at least one selected leader-converter can access the rated voltage references.

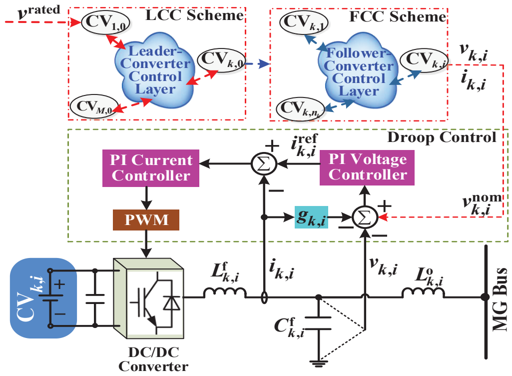

Fig. 1. Flowchart of the proposed strategy for a multiple dc MG cluster system.

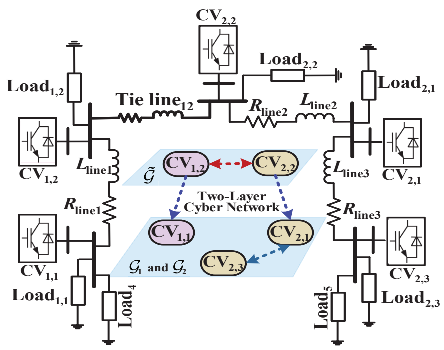

Fig. 2. Single line diagram of a multiple dc MG cluster system and the corresponding two-layer cyber network.

Now the proposed droop-based two-layer cooperative strategy, which is supported by a two-layer cyber network structure, can be drawn in Fig. 1. As seen, the LCC scheme is responsible for information exchange of all leader-converters from different MG clusters, to synchronize their weighted average voltage to v^{rated} as well as enable current sharing among multiple MG clusters. The operation states of each leader-converter, $\text{CV}_{k,0}$ $(k \in \mathcal{I}_M)$, can be accessed by its follower-converters, $\text{CV}_{k,i}$ $(i \in \mathcal{I}_{n_k})$, within the kth MG cluster in a distributed way. Based on this, the FCC scheme is responsible for information exchange of all follower-converters within each MG_k, to drive their weighted average voltage and current output ratios to that of their respective leader-converters, $\text{CV}_{k,0}$. Then, all the nominal set-points, $v_{k,i}^{\text{nom}}$ $(i \in \mathcal{I}_{n_k} \cup \{0\})$, generated through $\mathcal{G}_k$ and $\tilde{\mathcal{G}}$), will be locally transmitted to the voltage control loop of each converter's primary control stage. By employing the proportional-integral (PI) voltage and current controllers, the voltage loop provides reference values, $i_{k,i}^{\text{ref}}$, for the current loop, which finally calculates the current errors to regulate the duty cycle of the converter outputs by pulse width modulator (PWM) mode. Since the evolutions of FCC and LCC schemes may involve different time constants, τ and T, as shown in (5) and (6), they should be selected to satisfy the derived control condition (12), which will be verified in the next simulation section.

Table 1. Parameters for the test dc MG clusters

$\text{CV}_{1,1\&2,2}(i_{k,i}^{\max} = 2A)$		$\text{CV}_{1,2\&2,1\&2,3}(i_{k,i}^{\max} = 4A)$	
$V_{\text{DC}} = 180V,\ g_{k,i} = 6$		$V_{\text{DC}} = 150V,\ g_{k,i} = 3$	
$\text{Load}_{1,1\&1,2}$	$\text{Load}_{2,1}$	$\text{Load}_{2,2\&3,3\&4}$	Load_5
$0.35\ kW$	$0.5\ kW$	$0.4\ kW$	$0.6\ kW$
Line_1	Line_2	Line_3	TieLine_{12}
0.64Ω	0.51Ω	0.64Ω	1.15Ω
$1.32\ \mu H$	$1.05\ \mu H$	$1.32\ \mu H$	$2.37\ \mu H$

4. SIMULATION RESULTS

The effectiveness of the droop-based two-layer cooperative strategy is verified by simulating a multiple dc MG cluster system in MATLAB/SimPowerSystems. Fig. 2 shows the basic cyber-physical network topology structure of the system that includes two dc MG clusters, respectively, consisting of 2 and 3 converters and some local loads. MGs are connected through resistive-inductive lines. The lines between converters are modeled as series RL branches. The specifications of the converters, lines, and loads are summarized in Table I.

The desired rated voltage reference, v^{rated}, is set as 250V. Meanwhile, as seen in Fig. 2, we set $\text{CV}_{1,2}$ and $\text{CV}_{2,2}$ as the leader-converters from MG_1 and MG_2, respectively, and the adjacency matrices of the two-layer cyber network can be written as $A_1 = [0]$, $A_2 = [0, 1; 1, 0]$, $\tilde{A} = A_2$, and the leader-adjacency matrices are $B_1 = \mathrm{diag}\{1\}$, $B_2 = \mathrm{diag}\{1, 0\}$, and $\tilde{B} = B_2$. Obviously, $\varsigma = (1, 1, 1, 1, 1)^T$ and $\tilde{\varsigma} = (1, 1)^T$. Then $\mu_1 = (1)$, $\mu_2 = (1/2, 1/2)^T$, and $\tilde{\mu} = \mu_2$. By simple calculation, we obtain that $\lambda_{\min}(\mathrm{diag}(\varsigma)L + B) = 0.2679$, $\lambda_2(\mathrm{diag}(\tilde{\varsigma})\tilde{L}) = 2$, $\lambda_{\max}([\mathrm{diag}(\tilde{\varsigma})\tilde{L}]^2) = 4$, $\lambda_{\min}(\mathrm{diag}(\tilde{\varsigma})\tilde{L}+\tilde{B}) = 0.3820$, and $\lambda_{\max}([\mathrm{diag}(\tilde{\varsigma})\tilde{L}+\tilde{B}]^2) = 6.8541$. Thus the upper bound of τ/T can be calculated as $\vartheta = \min\{0.5359, 0.0597\} = 0.0597$. Next set the time constants as $\tau = 0.01$ and $T = 0.2$ to satisfy (12). The following simulation scenario proceeds as follows: 1) Stage 1: at $t = 0$s, MG_1 and MG_2 are in islanded mode with all loads except $\text{Load}_{4\&5}$. 2) Stage 2: at $t = 0.5$s, MG_1 and

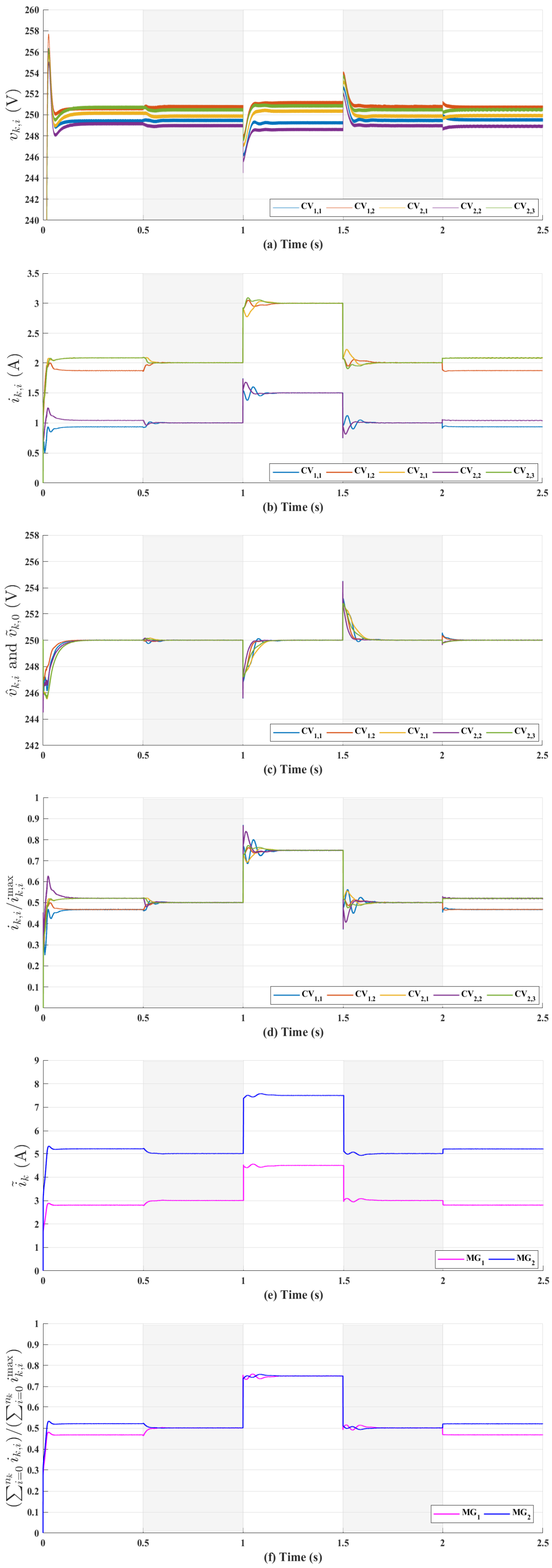

Fig. 3. Control performance of the proposed cooperative strategy: (a)-(c) voltage response, current outputs, and voltage estimates of all converters; (d) current output ratios of all converters; and (e)-(f) current outputs and ratios of the two MG clusters.

MG_2 are connected. 3) Stage 3: at $t = 1$s, $\mathrm{Load}_{4\&5}$ are added. 4) Stage 4: at $t = 1.5$s, $\mathrm{Load}_{4\&5}$ are removed. 5) Stage 5: at $t = 2$s, MG_1 and MG_2 are disconnected.

4.1 Control performance of the proposed strategy

The results in the proposed two-layer cooperative strategy are given in Fig. 3. As seen in Fig. 3(a), in each stage all converters' voltages can be regulated to an acceptable range, with their weighted average value converging to the rated references rapidly as shown in Fig. 3(c). The current outputs of all converters, drawn in Fig. 3(b), finally converge to two steady states since they have two different droop coefficients as set in Table I. The current output ratios of all converters are depicted in Fig. 3(d), which indicates that the current sharing objective among all converters within each MG clusters can be realized. Moreover, Figs. 3(e) and 3(f) draw all MG clusters' current outputs and output ratios evolution, which further verifies the realization of current sharing among multiple MG clusters. Thus the proposed strategy is effective for load change and also robust against MG plug and play operation.

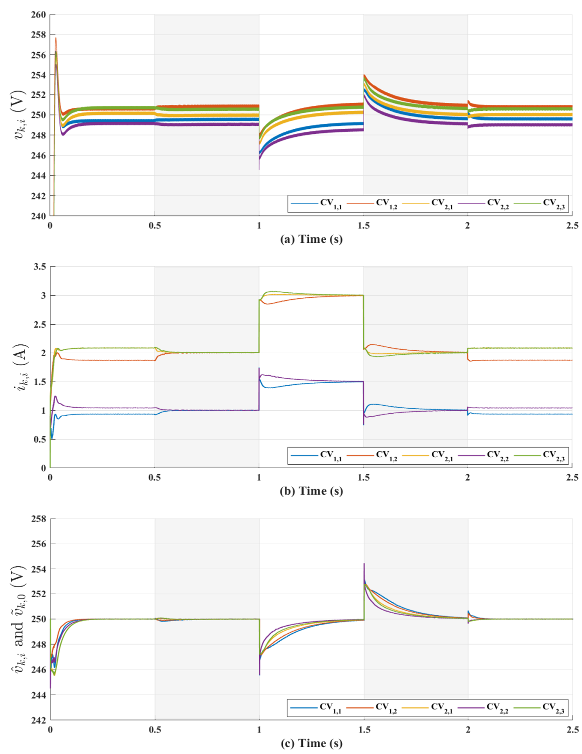

Fig. 4. Control performance of the existing cooperative strategies: (a)-(c) voltage response, current outputs, and voltage estimates of all converters.

4.2 Comparison with existing cooperative strategies

The comparison with the existing single-layer cooperative strategies is presented here [Lai (2016), Lu (2018)], the associated results are shown in Fig. 4. By comparing Figs. 3 and 4 as $t \in [0, 0.5) \cup [2, 2.5)$, it can be found that there is almost no difference for these two control strategies when each dc MG cluster is operated in islanded mode due to the same cyber network structure during this time period. However, when MG_1 and MG_2 are connected as

$t \in [0.5, 2)$, the better control performance of the proposed two-layer cooperative strategy shown in Fig. 3 becomes apparent than that shown in Fig. 4, especially for the load change period as $t \in [1.5, 2)$. By analysis, since the proposed strategy ensures the energy exchange among multiple MG clusters to be completed by directly feeding back the current sharing mismatches across the leader and follower control layers into the primary control stage, the corresponding time consumption can be then significantly reduced. It further indicates that the established sparse two-layer cyber network well fits the physical cluster topology structure of the multiple dc MG cluster.

5. CONCLUSION

A droop-based two-layer cooperative strategy has been established for multiple dc MG clusters, under which all converters' voltages can be regulated to an acceptable range and the accurate current sharing within each MG cluster and among multiple MG clusters can also be simultaneously achieved, as long as the control time constants of the established two-layer cyber network match the associated physical cluster topology structure of the multiple dc MG cluster. All the proposed fully distributed control schemes can be implemented in any sparse cyber networks.

ACKNOWLEDGEMENTS

This work was supported in part by the National Natural Science Foundation of China under Grant 61773158, in part by the Natural Science Foundation of Hunan Province under Grant 2018JJ2051, in part by the Fundamental Research Funds for the Central Universities under Grant 2042019kf0186, and in part by the Humboldt Research Council of Germany under Grant HB1807005.

REFERENCES

Yu, X., and Xue, Y. (2016). Smart grids: a cyber-physical systems perspective. *Proc. IEEE*, 104(5), 1058-1070.

Guerrero, J.M., Vasquez, J.C., Matas, J., Castilla, M., Vicuna, L.G.D., and Castilla, M. (2011). Hierarchical control of droop-controlled ac and dc microgrids-A general approach toward standardization. *IEEE Transactions on Industrial Electronics*, 58(1), 158-172.

Zhong, Q.C. (2011). Robust droop controller for accurate proportional load sharing among inverters operated in parallel. *IEEE Transactions on Industrial Electronics*, 60(4), 1281-1290.

Huang, P., Liu, P., Xiao, W., and Moursi, M. (2015). A novel droop-based average voltage sharing control strategy for dc microgrids. *IEEE Transactions on Smart Grid*, 6(2), 1096-1106.

Lai, J., Zhou, H., Lu, X., Yu, X., and Hu, W. (2016). Droop-based distributed cooperative control for microgrids with time-varying delays. *IEEE Transactions on Smart Grid*, 7(4), 1775-1789.

Nasirian, V., Shafiee, Q., Guerrero, J.M., Lewis, F.L., and Davoudi, A. (2016). Droop-free distributed control for ac microgrids. *IEEE Transactions on Power Electronics*, 31(2), 1600-1617.

Lu, X., Yu, X., Lai, J., Guerrero, J.M., and Wang, Y. (2018). A novel distributed secondary coordination control approach for islanded microgrids. *IEEE Transactions on Smart Grid*, 9(4), 2726-2740.

Farag, H.E., El-Saadany, E.F., and Seethapathy, R. (2012). A two ways communication-based distributed control for voltage regulation in smart distribution feeders. *IEEE Transactions on Smart Grid*, 3(1), 271-281.

Dam, D.H., and Lee, H.H. (2018). A power distributed control method for proportional load power sharing and bus voltage restoration in a dc microgrid. *IEEE Transactions on Industry Applications*, 54(4), 3616-3625.

Tucci, M., Meng, L., Guerrero, J.M., and Ferrari-Trecate, G. (2018). Stable current sharing and voltage balancing in DC microgrids: A consensus-based secondary control layer. *Automatica*, 95, 1-13.

Guo, F., Xu, Q., Wen, C., Wang, L., Wang, P. (2018). Distributed secondary control for power allocation and voltage restoration in islanded dc microgrids. *IEEE Transactions on Sustainable Energy*, 9(4), 1857-1869.

Cucuzzella, M., Trip, S., Persis, C.D., Cheng, X., Ferrara, A., and Schaft, A. (2018). A robust consensus algorithm for current sharing and voltage regulation in dc microgrids. *IEEE Transactions on Control Systems Technology*, 27(4), 1583-1595.

Dong, M., Li, L., Nie, Y., Song, D., and Yang, J. (2019). Stability analysis of a novel distributed secondary control considering communication delay in dc microgrids. *IEEE Transactions on Smart Grid*, 10(6), 1096-1106.

Lai, J., Lu, X., Yu, X., Monti, A., and Zhou, H. (2020). Distributed voltage regulation for cyber-physical microgrids with coupling delays and slow switching topologies. *IEEE Transactions on Systems Man and Cybernetics Part A-Systems and Humans*, 50(1), 100-110.

Shafiee, Q., Dragievi, T., Vasquez, J.C., and Guerrero, J.M. (2014). Hierarchical control for multiple DC microgrids clusters. *IEEE Transactions on Energy Conversion*, 29(4), 922-933.

Moayedi, S., and Davoudi, A. (2016). Distributed tertiary control of dc microgrid clusters. *IEEE Transactions on Power Electronics*, 31(2), 1717-1733.

Maknouninejad, A., Qu, Z., Enslin, J., and Kutkut, N. (2012). Clustering and cooperative control of distributed generators for maintaining microgrid unified voltage profile and complex power control. in *Proc. IEEE PES Transm. Distrib. Conf. Expo.*, 1-8.

Nutkani, I.U., Loh, P.C., and Blaabjerg, F. (2013). Distributed operation of interlinked ac microgrids with dynamic active and reactive power tuning. *IEEE Transactions on Industry Applications*, 49(5), 2188-2196.

Lu, X., Lai, J., Yu, X., Wang, Y., and Guerrero, J.M. (2018). Distributed coordination of islanded microgrid clusters using a two-layer intermittent communication network. *IEEE Transactions on Industrial Informatics*, 14(9), 3956-3969.

Lai, J., Lu, X., Yu, X., and Monti, A. (2019). Cluster-oriented distributed cooperative control for multiple ac microgrids. *IEEE Transactions on Industrial Informatics*, 15(11), 5906-5918.

Apostolopoulou, D., Sauer, P., and Domlnguez-Garcla, A. (2014). Automatic generation control and its implementation in real time. in *Hawaii International Conference on System Sciences (HICSS)*, Waikoloa.

Olfati-Saber, R., and Murrary, R.M. (2004). Consensus problems in networks of agents with switching topology and time-delays. *IEEE Transactions on Automation Control*, 49(9), 1520-1533.